PAPER NUMBER 61-PET-20

Deformation of Drill Pipe Held in Rotary Slips

T. VREELAND, JR.[1]

Associate Professor of
Mechanical Engineering,
California Institute of
Technology, Pasadena, Calif.

This paper presents an analysis of measurements of drill-pipe deformation in the slip area. Drill pipe was loaded in excess of the load at the minimum yield strength with the pipe in VARCO Type SDL and Type SDXL slips. A VARCO Type MSS solid master bushing was used with the type SDL slips and the master bushing of a VARCO KMPC unit was used with the Type SDXL slips. Measurements were made on the reduction in pipe diameter in the slip area as a function of load. Values of load which caused inelastic deformation of the pipe are determined and compared to the values previously calculated from theory.

1 Also, Consultant, Abegg and Reinhold Company, Los Angeles, Calif.

Contributed by the Petroleum Division for presentation at the Petroleum Mechanical Engineering Conference, Kansas City, Mo., September 24-27, 1961, of The American Society of Mechanical Engineers. Manuscript received at ASME Headquarters, August 7, 1961.

Written discussion on this paper will be accepted up to October 27, 1961.

Copies will be available until July 1, 1962.

Deformation of Drill Pipe Held in Rotary Slips

T. VREELAND, JR.

As drilling depths continually increase and hydraulic efficiency demands the use of $4\frac{1}{2}$ or 5-in-OD drill pipe down to completion depth, the vastly greater hook loads now encountered are bringing attention to drill-pipe failures occurring in the slip area. A closer examination and analysis of these failures has revealed that they are generally being caused by worn rotary slips and master bushings, especially conventional split-type master bushings. In addition, improperly repaired rotary slips and master bushings, resharpened gripping elements, and poor handling techniques also contribute unnecessary damage in the slip area of drill pipe.

Today many deep wells are being drilled using proper rotary slips and solid-type master bushings with no evidence of damage or failure in the slip area of the drill pipe. This is unquestionably the result of close supervision coupled with intelligent and periodic maintenance.

There is still a considerable number of rotary rigs drilling medium or deep holes utilizing conventional rotary slips in standard split-type master bushings. Fig.1 illustrates the effect on drill pipe when handled by conventional rotary slips set in worn split master bushings in a worn rotary table. This condition has been responsible for a large amount of damage to drill pipe in the slip area.

For this testing program it was decided to use VARCO Type SDL long rotary slips in a VARCO Type MSS solid master bushing complete with API insert bowls, as well as VARCO Type SDXL extra long rotary slips in a master bushing of a VARCO Type KMPC unit which has an extended API bowl taper. Fig.2 illustrates the Type SDL Rotary Slip set on 5-in-OD drill pipe in the Type MSS solid master bushing. Fig.3 illustrates the Type SDXL rotary slip set on 5-in-OD drill pipe in the master bushing of a KMPC unit. The extra long slip fully backed up by the extended API bowl provides a much greater backed-up area of the gripping elements when they hold drill pipe. This means that

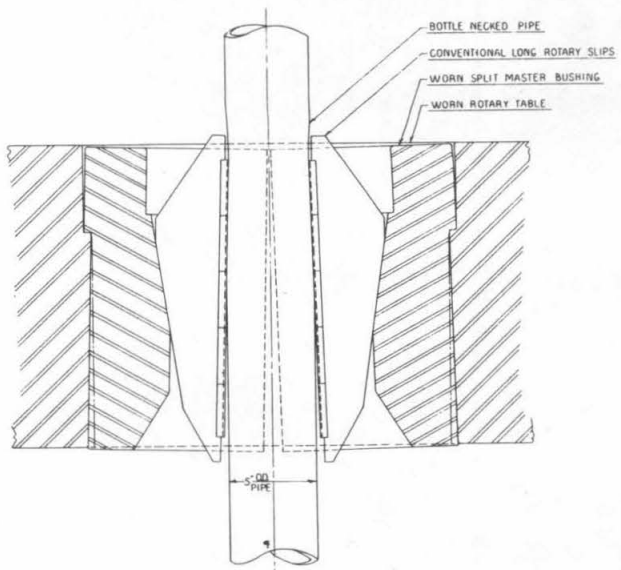

Fig. 1 Cross section of API rotary slips set on 5-in-OD drill pipe in a standard split master bushing indicating wear

the transverse load or compressive force on the drill pipe by the slips when excessive hook loads prevail will be more uniformly distributed throughout the slip area of the drill pipe. Accordingly, there cannot be a concentration of load as is the case in Fig.1 when split-type master bushings are used. It will be shown that the collapse strength of Grade "E" drill pipe in the slip area is considerable and that under correct conditions crushing will not occur even though hook loads in excess of 500,000 lb are brought to bear on the drill pipe.

TEST APPARATUS AND PROCEDURE

The loading system consisted of a piston mandrel combination, schematically shown in Fig.4. Four displacement gages (U-gages which employ SR-4 strain gages) were mounted on the interior of the drill pipe in the slip area to measure changes in pipe diameter. Type SR-4 strain gages were mounted on the drill pipe below the slip area to measure axial strain. The gages were connected in conventional Wheatstone bridge circuits, and the bridge output was indicated by a galvanometer. Suitable switching, calibration, and zeroing circuits permitted determination of the reduction in pipe diameter and the axial strain in the pipe below the slips. The bottom of each drill pipe specimen was thread-connected to the piston mandrel and the upper section was held in the slips. A minimum of two pipe diameters was maintained be-

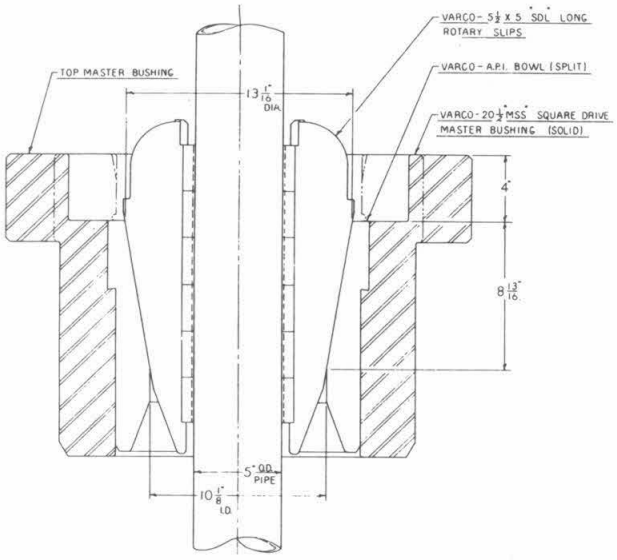

Fig. 2 Cross section of VARCO Type SDL rotary slips complete with 5 1/2 x 5-in. inserts set on 5-in-OD drill pipe in a VARCO Type MSS solid master bushing

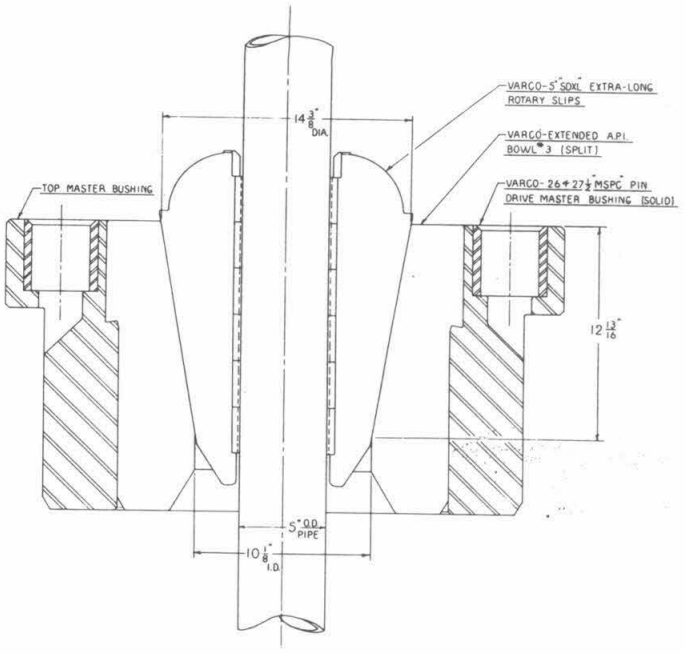

Fig. 3 Cross section of VARCO Type SDXL rotary slips complete with 5-in. inserts set on 5-in-OD drill pipe in a master bushing of a KMPC unit

tween the upset in the pipe at the threaded connection and the bottom of the slips, and also between the top of the slips and the top of the pipe. Drill-pipe specimens were loaded in increments of approximately 25,000 or 50,000 lb by application of hydraulic pressure to the annulus above the loading piston. Readings of diameter reduction and axial strain in the pipe were taken at each load. The outside-diameter profile of the pipe specimens was measured by a micrometer caliper before and after loading.

Test Specimens

Two test specimens, marked Nos. 1 and 2, were machined from SAE 4130 normalized 5-in. tubing to the nominal inside diameter of 5 in., 19.5 lb/ft drill pipe. These specimens were used in preliminary tests to check out the testing procedures. Four test specimens of 5 in., 19.5 lb/ft grade E drill pipe, supplied by Youngstown, were marked Nos. 3, 4, 5, and 6. The test specimens were loaded under the conditions given in Table 1. Because of the limited number of Youngstown pipe specimens, two tests were made on each specimen. The top 15 in. of pipe was cut off after the first pull on each specimen, so that the displacement gages could be replaced 15 in. below their previous position. The 16-in-long gripping faces of the slip therefore overlapped by 1 in. the area that was gripped on the first pull.

Data Reduction

The galvanometer deflection is converted to

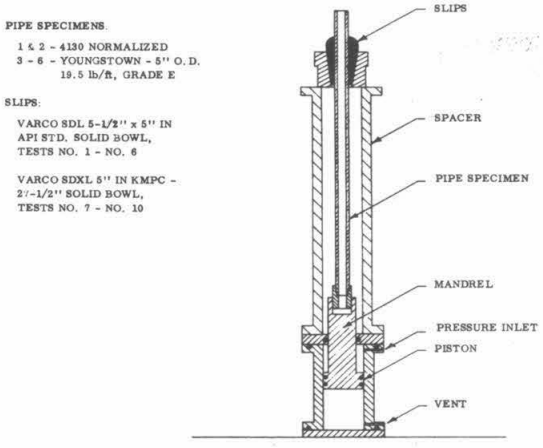

Fig. 4 Schematic diagram of loading system

reduction in pipe diameter (signal from deflection gages in pipe ID), or tensile stress in the pipe (signal from axial strain gages mounted on the drill pipe) with the aid of the calibration curves. The tensile load on the pipe was taken as the product of the hydraulic pressure and the area of the annulus above the piston.

A plot of load versus diameter reduction at the four gage locations in the slip area was made for each test. The data for each plot were analyzed in the following manner:

(a) Points which were obviously inconsistent with the trend of the data were discarded.

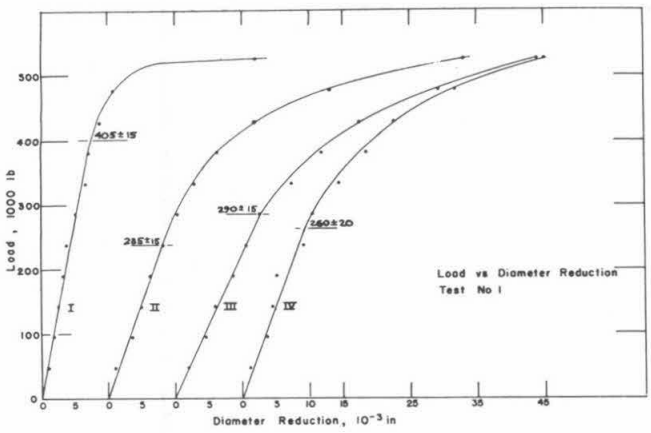

Fig. 5 Load versus diameter reduction, Test No. 1

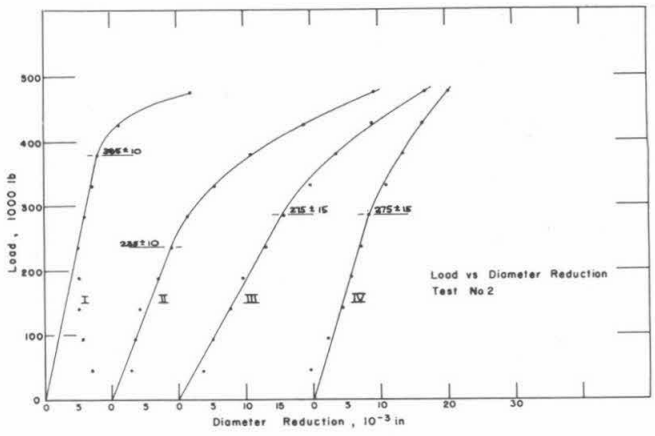

Fig. 6 Load versus diameter reduction, Test No. 2

Table 1 Test Conditions and Gage Locations

Test Number	Specimen Number	Type of Slips	Lubrication of Bowl	Location of Displacement Gages above Bottom of Slips, in.				Location of Strain Gages Below Bottom of Slips, in.
				I	II	III	IV	
1	1	SDL	Best-O-Life	0	3	6	9	--
2	2	SDL	Best-O-Life	0	3	6	9	--
3	3	SDL	Jet Lube 21	0	5	10	15	26
4	3	SDL	Jet Lube 21	0	5	10	15	11
5	4	SDL	Dry	0	5	10	15	26
6	4	SDL	Dry	0	5	10	15	11
7	5	SDXL	Dry	0	5	10	15	26
8	5	SDXL	Dry	0	5	10	15	11
9	6	SDXL	Jet Lube 21	0	5	10	15	26
10	6	SDXL	Jet Lube 21	0	5	10	15	11

(b) The points in the linear load versus deflection range were divided into two groups. Each group of points was averaged to give a load and a deflection value.

(c) The slope of the linear portion of the curve was calculated from the two average points found in (b). The line between average points was taken as the "best-fit line" for the linear portion of the data and the deflection readings were zero corrected as indicated by the intercept of the best fit curve and the zero load axis.

(d) The zero corrected data were plotted, and a curve was fitted to the points beyond the linear range.

(e) The load at the first deviation from linearity was determined. It is assumed that this load is equal to the load at the onset of yielding at the particular gage location. The uncertainty in the yield load was estimated taking into account the shape of the load-deflection curve, and the scatter in the test points in the vicinity of the yield load.

(f) The load at an offset of 0.005 in. from the linear slope was determined. It is assumed that this load is equal to the load required to produce a permanent reduction in pipe diameter of 0.005 in.

(g) The permanent reduction in diameter produced by the loading was determined by (1) assuming that the unloading curve followed the slope of the initial linear portion of the curve, (2) by taking the reading of the deflection gage at the completion of the test when the load was removed, and (3) by taking the difference in micrometer caliper readings of the specimens, before and after loading.

The elastic limit of the pipe was determined from a plot of load versus axial strain. The axial strain was determined by dividing the axial stress by the modulus 30×10^6 psi. The value of

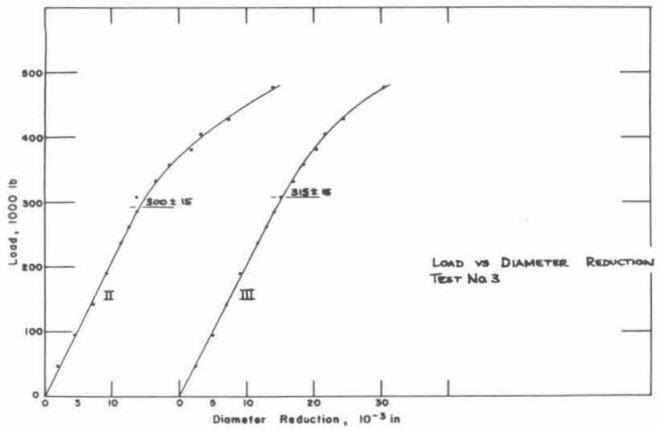

Fig. 7 Load versus diameter reduction, Test No. 3

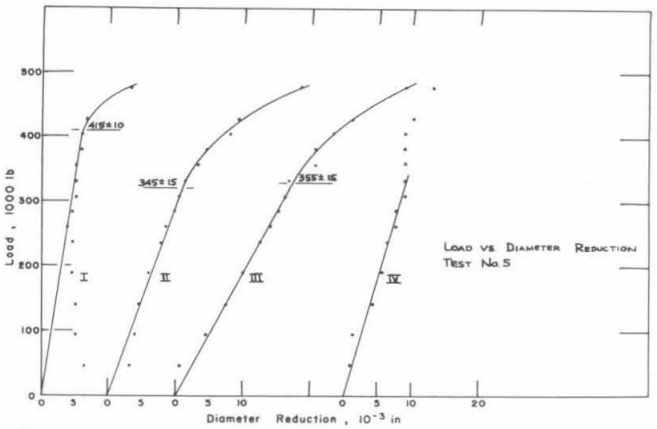

Fig. 9 Load versus diameter reduction, Test No. 5

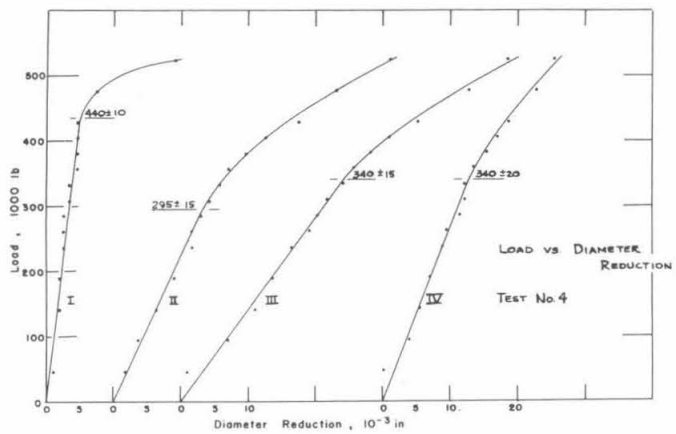

Fig. 8 Load versus diameter reduction, Test No. 4

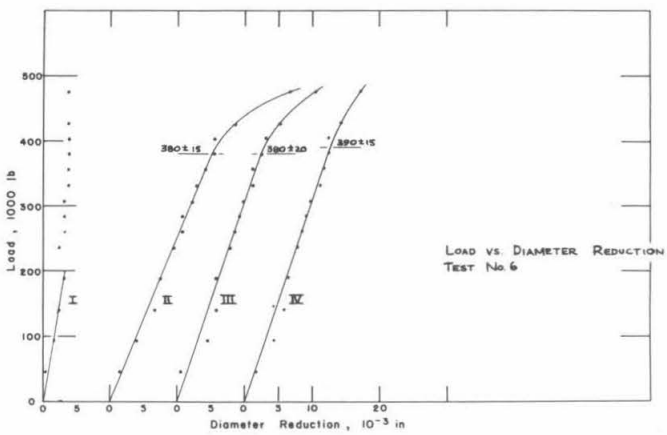

Fig. 10 Load versus diameter reduction, Test No. 6

strain, at the first deviation from linearity, multiplied by 30 x 10^6 psi is taken as the elastic limit of the pipe.

The data reduction calculations are presented in Tables 2 through 11. A summary of test results is given in Table 12. The reduced data are plotted on Figs.5 through 14, which give load versus diameter reduction. Figs.15 and 16 give load versus axial strain.

DISCUSSION OF TEST DATA

The two tests on each of the Youngstown specimens show consistent results, values of load at the first inelastic deformation agree within the experimental uncertainty. The location of the first inelastic deformation of the pipe in the slip area followed a consistent pattern in the tests. The following observations are made in comparing the tests with SDL and SDXL slips:

1 Tests Nos. 1 through 6 show that the first inelastic deflections occur with the SDL slips in the lower section of the gripped area of the pipe. Tests Nos. 7 through 10 with the SDXL slips show that the first inelastic deflections occur in the upper section of the gripped area of the pipe.

2 Under similar conditions pipe held in SDL and SDXL slips exhibits inelastic deformation at essentially the same load.

3 Higher loads are required to produce inelastic deformation with SDL and SDXL slips when the bowls are dry rather than lubricated.

4 An increase in load of 100,000 lb over the yield load produces less than 0.005 in. permanent deformation with SDL and SDXL slips in lubricated bowls.

The maximum permanent reduction in pipe diameter is given in Table 13. The permanent deformation determined by assuming unloading at the slope of the initial loading is the most reliable. The

TABLE 2

U - GAGES

HYD PRESS psi x 10^2	LOAD lb. x 10^3	I GALV DIV.	I in. x 10^{-3}	I Zero corrected in x 10^{-3}	II GALV DIV.	II in. x 10^{-3}	II Zero corrected in x 10^{-3}	III GALV DIV.	III in. x 10^{-3}	III Zero corrected in x 10^{-3}	IV GALV DIV.	IV in. x 10^{-3}	IV Zero corrected in x 10^{-3}
5	47.6	-1	1.3	1.2	-2	2.7	1.0	-2	2.7	2.0	-4	5.3	1.1
10	95.2	-1.5	2.0	1.9	-4	5.3	3.6	-4	5.3	4.6	-6	8	3.8
15	142.8	-2	2.7	2.6	-5	6.7	5.0	-5	6.7	6.0	-6.5	8.7	4.5
20	190.4	-2.5	3.3	3.2	-6	8	6.3	-7	9.3	8.6	-7	9.3	5.1
25	238.0	-3	4	3.9	-7.5	10.0	8.3	-8.5	11.4	10.7	-10	13.3	9.1
30	285.6	-4	5.3	5.2	-9	12.0	10.3	-10	13.3	12.6	-11	14.7	10.5
35	333.2	-5	6.7	6.6	-11	14.7	13.0	-13.5	18.0	17.3	-14	18.7	14.5
40	380.8	-5.5	7.3	7.2	-13.5	18.0	16.3	-17	22.7	22.0	-17	22.7	18.5
45	428.4	-6.5	8.7	8.6	-17.5	23.4	21.7	-21	28.0	27.3	-20	26.7	22.5
50	476.0	-8	10.7	10.6	-26	34.7	33.0	-30	40.0	39.3	-27	36.0	31.8
55	523.6	-24	32.0	31.9	-41	54.7	53.0	-41	54.7	54.0	-37	49.4	45.2
Zero Correction Factor x 10^{-3} in.		-0.1			-1.7			-0.7			-4.2		
Slope Linear Curve KIPS/10^{-3} in.		54.5			28.6			21.9			28.6		

Points averaged to determine linear curve.

TABLE 3

U - GAGES

HYD PRESS psi x 10^2	LOAD lb. x 10^3	I GALV DIV.	I in. x 10^{-3}	I Zero corrected in x 10^{-3}	II GALV DIV.	II in. x 10^{-3}	II Zero corrected in x 10^{-3}	III GALV DIV.	III in. x 10^{-3}	III Zero corrected in x 10^{-3}	IV GALV DIV.	IV in. x 10^{-3}	IV Zero corrected in x 10^{-3}
5	47.6	+2	-2.7	(7.2)	-.5	0.7	2.9]	-6	8	(3.6)	-1.5	2.0	(-.3)
10	95.2	+3	-4	(5.9)	-1	1.3	3.5]	-7	9.3	4.9]	-3.5	4.7	2.4]
15	142.8	+3.5	-4.7	(5.2)	-1.5	2.0	4.2]	-9	12	7.6]	-5	6.7	4.4]
20	190.4	+3.5	-4.7	(5.2)	-3.5	4.7	6.9]	-10.5	14	9.6]	-6	8	5.7]
25	238.0	+3.5	-4.7	5.2]	-5	6.7	8.9]	-13	17.3	12.9]	-7	9.4	7.1]
30	285.6	+3	-4	5.9]	-7	9.4	11.6	-15	20	15.6]	-8	10.7	8.4]
35	333.2	+2	-2.7	7.2]	-10	13.3	15.5	-18	24	19.6	-10	13.3	11
40	380.8	+1.5	-2	7.9]	-14	18.7	20.9	-21	28	23.6	-12	16	13.7
45	428.4	-1	+1.3	11.2	-20	26.7	28.9	-25	33.4	29.0	-14	18.7	16.4
50	476.0	-9	12	21.9	-28	37.4	39.6	-31	41.3	36.9	-17	22.7	20.4
55	523.6	-10	13.3	(23.2)	-30	40	(42.2)	-32	42.7	(38.3)	-17.5	23.4	(21.1)
60	571.2	-10.5	14	(23.9)	-30	40	(42.2)	-33	44	(39.6)	-18	24	(21.7)
Zero Correction Factor x 10^{-3} in.			+9.9			+2.2			-4.4			-2.3	
Slope Linear Curve KIPS / 10^{-3} in.			47.6			26.5			18.9			34.0	

] ⟹ Points averaged to determine linear curve.

( ) ⟹ Discarded points.

TABLE 4
U - GAGES

HYD PRESS. psi x 10^2	LOAD lb. x 10^3	I GALV DIV.	I in. x 10^{-3}	I Zero corrected inx10^{-3}	II GALV DIV.	II in. x 10^{-3}	II Zero corrected inx10^{-3}	III GALV DIV.	III in. x 10^{-3}	III Zero corrected inx10^{-3}	IV GALV DIV.	IV in. x 10^{-3}	IV Zero corrected inx10^{-3}	V & VI AV. GALV DIV.	V & VI Axial Strain, %
5	47.6	+2			-1	1.3	1.8	-4	5.3	2.3	-1			+10.3	.021
10	95.2	+1.5			-3	4	4.5	-6	8	5.0	-1			+21.5	.054
15	142.8	+1.5			-5	6.7	7.2	-7.5	10	7	-1.5			+31.5	.079
20	190.4	+1			-6.5	8.7	9.2	-9	12	9	-2			+41.5	.106
25	238.0	+1			-8	10.7	11.2	-11	14.7	11.7	-2			+13x4	.13
27.5	261.8	0			-9	12	12.5	-12	16	13	-3			+14.5x4	.145
30	285.6	0		Discarded Data	-10	13.3	13.8	-13	17.3	14.3	-3		Discarded Data	+15.5x4	.155
32.5	309.4	0			-10	13.3	(13.8)	-13.5	18	15	-3.5			+16.5x4	.165
35	333.2	0			-12	16	16.5	-15	20	17	-4			+17.8x4	.178
37.5	357.0	+.5			-13.5	18	18.5	-16	21.4	18.4	-4			+19x4	.19
40	380.8	+.5			-16	21.3	21.8	-17.5	23.3	20.3	-4.5			+20.5x4	.205
42.5	404.6	+.5			-17	22.6	23.1	-18.5	24.6	21.6	-4.5			+21.3x4	.213
45	428.4	+.5			-20	26.7	27.2	-20.5	27.4	24.4	-5			+23.3x4	.233
50	476.0	-2			-25	33.4	33.9	-25	33.4	30.4	-6.5			+26.3x4	.263
Zero Correction Factor x 10^{-3} in.						+0.5			-3.0					(GALV. DIVx4)(10^{-4})= ϵ	
Slope Linear Curve KIPS / 10^{-3} in.						21			20			(63.4)		(GALV. DIV)($\frac{1}{4} \cdot 10^{-4}$)= ϵ	

]⇒ Points averaged to determine linear curve

( )⇒ Discarded points

TABLE 5
U - GAGES

HYD PRESS psi x 10^2	LOAD lb. x 10^{-3}	I GALV DIV.	I in. x 10^{-3}	I Zero corrected in x 10^{-3}	II GALV DIV.	II in. x 10^{-3}	II Zero corrected in x 10^{-3}	III GALV DIV.	III in. x 10^{-3}	III Zero corrected in x 10^{-3}	IV GALV DIV.	IV in. x 10^{-3}	IV Zero corrected in x 10^{-3}	V & VI AV. GALV DIV.	V & VI Axial Strain, %
5	47.6	0	0	.7	- .5	0.7	1.7	-2.5	3.3	(1)	-1	1.3	(.1)	+10.5	.026
10	95.2	+ .5	-0.7	(-1.4)	-2	2.7	3.7	-7	9.3	7.0	-4	5.3	4.1	+22	.055
15	142.8	-1	1.3	2.0	-4	5.3	6.3	-10	13.3	11.0	-5	6.7	5.5	+33	.082
20	190.4	-1	1.3	2.0	-6	8	9	-12	16	13.7	-6	8	6.8	+44	.11
25	238.0	-1.5	2.0	2.7	-8	10.7	11.7	-14	18.7	16.4	-7.5	10	8.8	+13x4	.13
27.5	261.8	-1.5	2.0	2.7	-8	10.7	11.7	-16	21.4	19.1	-8	10.7	9.5	+14x4	.14
30	285.6	-1.5	2.0	2.7	-9	12	13	-17	22.6	20.3	-9.5	12.7	11.5	+15.3x4	.153
32.5	309.4	-2	2.7	3.4	-10	13.3	14.3	-18	24	21.7	-10	13.3	12.1	+16.7x4	.167
35	333.2	-3	2.7	3.4	-11	14.7	15.7	-20	26.6	24.3	-10	13.3	12.1	+18x4	.18
37.5	357.0	-3	4	4.7	-12	16	17	-21	28	25.7	-11	14.7	13.5	+19.5x4	.195
40	380.8	-3	4	4.7	-14	18.7	19.7	-23	30.6	28.3	-12.5	16.7	15.5	+21x4	.21
42.5	404.6	-3	4	4.7	-16	21.4	22.4	-25	33.4	31.1	-13.5	18	16.8	+22x4	.22
45	428.4	-3	4	4.7	-20	26.6	27.6	-28	37.4	35.1	-15	20	18.8	+23.7x4	.237
50	476.0	-5	6.7	7.4	-24	32	33	-34	45.3	43	-18	24	22.8	+28x4	.28
55	523.6	-14	18.7	19.4	-30	40	41	-38	50.7	48.4	-20	26.6	25.4		
0	0	-12.5	16.7	17.4	-22	29.4	39.4	-22	29.4	27.1	-10	13.3	12.1		
Zero Correction, 10^{-3} in.		+0.7			+ 1			-2.3			- 1.2				
Slope, KIPS/10^{-3} in.		87.1			22.1			13.9			26.1				

( ) ⇒ Discarded points

] ⇒ Points averaged to determine linear curve

TABLE 6

U - GAGES

HYD PRESS psi x 10^2	LOAD lb. x 10^{-3}	I GALV DIV.	I in. x 10^{-3}	I Zero corrected in x 10^{-3}	II GALV DIV.	II in. x 10^{-3}	II Zero corrected in x 10^{-3}	III GALV DIV.	III in. x 10^{-3}	III Zero corrected in x 10^{-3}	IV GALV DIV.	IV in. x 10^{-3}	IV Zero corrected in x 10^{-3}	VI AV. GALV DIV.	VI Axial Strain, %
5	47.6	+1	-1.3	(6.6)	0	0	(3.2)	-6	8	(.7)	-4	5.3	0.9	+12	.03
10	95.2	+2	-2.7	(5.2)	- .5	.7	3.9	-9	12	4.7	-5	6.7	2.3	+21	.052
15	142.8	+2	-2.7	(5.2)	-1	1.3	4.5	-11	14.7	7.4	-6.5	8.7	4.3	+30	.075
20	190.4	+2.5	-3.3	(4.6)	-2	2.7	5.9	-13	17.3	10.0	-7.5	10	5.6	+42	.105
25	238.0	+2.5	-3.3	(4.6)	-3.5	4.7	7.9	-15	20	12.7	-8	10.7	6.3	+52	.13
27.5	261.8	+3	-4	(3.9)	-4	5.3	8.5	-16	21.4	14.1	-9	12	7.6	+15x4	.15
30	285.6	+2.5	-3.3	(4.6)	-5	6.7	9.9	-17	22.6	15.3	-9	12	7.6	+15x4	.15
32.5	309.4	+2	-2.7	(5.2)	-5.5	7.3	10.5	-17.5	23.4	16.1	-10	13.3	8.9	+17x4	.17
35	333.2	+2	-2.7	(5.2)	-6	8	11.2	-18	24	16.7	-10	13.3	(8.9)	+18x4	.18
37.5	357.0	+2	-2.7	5.2	-7.5	10	13.2	-21	28	(20.7)	-10	13.3	(8.9)	+20x4	.20
40	380.8	+1.5	-2	5.9	-8.5	11.3	14.5	-21	28	20.7	-10	13.3	(8.9)	+20.5x4	.205
42.5	404.6	+1.5	-2	5.9	-11	14.7	17.9	-23	30.6	23.3	-10	13.3	(8.9)	+24x4	.225
45	428.4	+1	-1.3	6.6	-12	16	19.2	-25	33.4	26.1	-11	14.7	(10.3)	+32x4	.24
50	476.0	-4	+5.3	13.2	-19	25.3	28.5	-31	41.3	34.0	-13	17.3	(12.9)	+20x4	.32
0	0	-4.5	+6	(13.9)	-12.5	16.7	19.9	-17	22.6	15.3	-6	8	(3.6)		.20
Zero correction Factor x 10^{-3} in.			+7.9			+3.2			-7.3			-4.4			
Slope linear Curve KIPS/10^{-3} in.			67.6			29.7			19.2			36.2			

] ⇒ Points averaged to determine linear curve

( ) ⇒ Discarded points

TABLE 7

U - GAGES

HYD PRESS psi x 10^2	LOAD lb. x 10^3	I GALV DIV.	I in. x 10^{-3}	I Zero corrected in x 10^{-3}	II GALV DIV.	II in. x 10^{-3}	II Zero corrected in x 10^{-3}	III GALV DIV.	III in. x 10^{-3}	III Zero corrected in x 10^{-3}	IV GALV DIV.	IV in. x 10^{-3}	IV Zero corrected in x 10^{-3}	V & VI GALV DIV.	V & VI Axial Strain, %
5	47.6	0	0	0.5	-3	4	1.5	-7	9.3	0.5	-2	2.7	1.8	+12	.03
10	95.2	-1	1.3	1.8	-5	6.7	(4.2)	-10	13.3	(4.5)	-4	5.3	(4.4)	+24	.06
15	142.8	-1.5	2.0	2.5	-7	9.3	(6.8)	-11	14.7	(5.9)	-5	6.7	(5.8)	+35	.087
20	190.4	-2	2.7	3.2	-7.5	10	7.5	-11	14.7	5.9	-5.5	7.3	6.4	+45	.112
25	238.0	-1.5	2.0	(2.5)	-9	12	9.5	-12.5	16.7	7.9	-6.5	8.7	7.8	+14.5x4	.145
27.5	261.8	-2	2.7	(3.2)	-10	13.3	10.8	-13	17.3	8.5	-7	9.3	8.4	+16x4	.16
30	285.6	-2	2.7	(3.2)	-10	13.3	10.8	-13.5	18	9.2	-7.5	10	9.1	+17x4	.17
32.5	309.4	-2	2.7	(3.2)	-11	14.7	12.2	-14	18.7	9.9	-8	10.7	9.8	+19.5x4	.195
35	333.2	-2.5	3.3	(3.8)	-11.5	15.3	12.8	-15	20	11.2	-9	12	11.1	+20.5x4	.205
37.5	357.0	-2.5	3.3	(3.8)	-12.5	16.7	14.2	-15	20	11.2	-9.5	12.7	11.8	+21.5x4	.215
40	380.8	-2.5	3.3	(3.8)	-13.5	18	15.5	-16	21.3	12.5	-10	13.3	12.4	+24x4	.24
42.5	404.6	-2.5	3.3	(3.8)	-13.5	18	(15.5)	-16.5	22	(13.2)	-10	13.3	(12.4)	+25x4	.25
45	428.4	-2.5	3.3	(3.8)	-16	21.3	18.8	-18	24	15.2	-11.5	15.3	14.4	+26.5x4	.265
50	476.0	-2.5	3.3	(3.8)	-22	29.3	26.8	-22	29.3	20.5	-13.5	18	17.1	+43.5x4	.435
0	0	+2	-2.7	(-2.2)	-14.5	19.3	16.8	-13	17.3	8.5	-6	8	7.1	+15x4	.15
Zero correction Factor x 10^{-3} in.			+0.5			-2.5			-8.8			-0.9			
Slope linear Curve KIPS / 10^{-3} in.			59.5			25.4			30.8			30.8			

⟹ Points averaged to determine linear curves.

( ) ⟹ Discarded points

TABLE 8

U - GAGES

HYD PRESS psi x 10^2	LOAD lb. x 10^3	I GALV DIV.	I in. x 10^{-3}	I Zero corrected in x 10^{-3}	II GALV DIV.	II in. x 10^{-3}	II Zero corrected in x 10^{-3}	III GALV DIV.	III in. x 10^{-3}	III Zero corrected in x 10^{-3}	IV GALV DIV.	IV in. x 10^{-3}	IV Zero corrected in x 10^{-3}	V & VI AV. GALV DIV.	V & VI Axial Strain, %	VII AV. GALV DIV.	VII Axial Strain, %	Dia. Reduction
5	47.6				+1	-1.3	(6.5)	+ .5	- .7	+ .9	+1.5	-2	.7	+ 7.5	.019	+ 8.5	.021	
10	95.2	Dead			+2	-2.7	(5.1)	0	0	1.6	+1	-1.3	1.4	+18	.045	+18	.045	
15	142.8				+2	-2.7	(5.1)	0	0	1.6	0	0	2.7	+28.5	.071	+26	.065	
20	190.4				+2.5	-3.3	(4.5)	+1	1.3	2.9	-1	+1.3	4.0	+40.5	.101	+36	.09	
25	238.0				+1.5	-2.0	(5.8)	-1.5	2.0	3.6	-1.5	2.0	4.7	+13x4	.13	+11.5x4	.115	
27.5	261.8				+2.0	-2.7	5.1	-1.5	2.0	3.6	-1.5	2.0	4.7	+13.7x4	.137	+12x4	.12	
30	285.6				+2	-2.7	5.1	-2	2.7	4.3	-2	2.7	5.4	+15.5x4	.155	+13	.13	
32.5	309.4				+1	-1.3	6.5	-2	2.7	4.3	-1.5	2.0	(4.7)	+16.7	.167	+14	.14	
35	333.2				+1	-1.3	6.5	-2.5	3.3	4.9	-2.5	3.3	6	+18.3	.183	+15	.15	
37.5	357.0				+1	-1.3	6.5	-3	4	5.6	-3	4	6.7	+18.5	.185	+16	.16	
40	380.8				0	0	7.8	-3.5	4.7	6.3	-3.5	4.7	7.4	+21	.21	+17.5	.175	
42.5	404.6				0	0	7.8	-4.5	6	7.6	-4	5.3	8.0	+22.3	.223	+18.5	.185	
45	428.4				- .5	+ .7	8.5	-5	6.7	8.3	-4.5	6	8.7	+24	.24	+20	.20	
47.5	452.2				-1.5	+2	9.8	-5.5	7.3	8.9	-5	6.7	9.4	+25	.25	+20	.20	
50	476.0				-4	5.3	13.1	-8.5	11.3	12.9	-6.5	8.7	11.4	+28.5	.285	+21	.21	
55	523.6				-15	20	27.8	-15	20	21.6	-10.5	14	16.7			+43	.43	
0	0				-13.5	18	25.8	-15	20	21.6	-9	12	14.7			+16.5	.165	
Zero Correction Factor, x 10^{-3} in.					+7.8			+1.6			+2.7							
Slope, Linear Curve KIPS/10^{-3} in.					52.8			69.5			53.8							

⟹] Points averaged to determine linear curve.

(⟹ Discarded points.

TABLE 9

U - GAGES

HYD PRESS psi x 10^2	LOAD lb. x 10^3	I GALV DIV.	I in. x 10^{-3}	I Zero corrected in x 10^{-3}	II GALV DIV.	II in. x 10^{-3}	II Zero corrected in x 10^{-3}	III GALV DIV.	III in. x 10^{-3}	III Zero corrected in x 10^{-3}	IV GALV DIV.	IV in. x 10^{-3}	IV Zero corrected in x 10^{-3}	V AV. GALV DIV.	V Axial Strain, %
5	47.6	+ .5		Discarded Data	-2	2.7	1.3	-4	5.3	2.8	-1.5	2	3.6	+12.5	.031
10	95.2	- .5			-4	5.3	3.9	-5	6.7	4.2	-2	2.7	4.3	25	.062
15	142.8	- .5			-5.5	7.3	5.9	-6.5	8.7	6.2	-2.5	3.3	4.9	38	.095
20	190.4	- .5			-6.5	8.7	7.3	-8	10.7	8.2	-3.5	4.7	6.3	52	.13
25	238.0	- .5			-7	9.3	7.9	-10	13.3	10.8	-5	6.7	8.3	16x4	.16
27.5	261.8	- .5			-9	12	10.6	-10	13.3	10.8	-5	6.7	8.3	17.5	.175
30	285.6	- .5			-9	12	10.6	-11	14.7	12.2	-6	8	9.6	20	.20
32.5	309.4	- .5			-10	13.3	11.9	-12	16	13.5	-7.5	10	11.6	22	.22
35	333.2	- .5			-10	13.3	11.9	-13	17.3	14.8	-8	10.7	12.3	23	.23
37.5	357.0	-1			-11	14.7	13.3	-13.5	18	15.5	-8.5	11.3	12.9	23.5	.235
40	380.8	-1			-12	16	14.6	-15	20	17.5	-10	13.3	14.9	27	.27
42.5	404.6	-1.5			-12	16	14.6	-15	20	17.5	-10	13.3	14.9	28.5	.285
45	428.4	-2			-15.5	20.7	(19.3)	-16	21.3	18.8	-11.5	15.3	16.9	30.5	.305
47.5	452.2	-2			-13.5	18	16.6	-16	21.3	18.8	-11.5	15.3	16.9	33	.33
50	476.0	-2			-15	20	18.6	-18	24	21.5	-13.5	18	19.6	35	.35
52.5	499.8	-2			-15	20	18.6	-18	24	21.5	-13.5	18	19.6	37	.37
55	523.6	-3			-16.5	22	20.6	-20	26.7	24.2	-15	20	21.6	42	.42
0	0	-4.5			-17.5	23.3	(21.9)	-19	25.3	22.8	-12	16	17.6	22x1	.055
Zero Correction Factor x 10^{-3} in.			--			-1.4			-2.5			+1.6			
Slope Linear Curve KIPS/10^{-3} in.			--			26.8			22.7			27.2			

⇒ Points averaged to determine linear curve.

( ) ⇒ Discarded points.

TABLE 10

U - GAGES

HYD PRESS psi 10^2	LOAD lb. 10^3	I GALV DIV.	I in. x 10^{-3}	I Zero corrected in x 10^{-3}	II GALV DIV.	II in. x 10^{-3}	II Zero corrected in x 10^{-3}	III GALV DIV.	III in. x 10^{-3}	III Zero corrected in x 10^{-3}	IV GALV DIV.	IV in. x 10^{-3}	IV Zero corrected in x 10^{-3}	V & VI AV. GALV DIV.	V & VI Axial Strain, %
5	47.6	-2	2.7	- .3	-3	4	1.5	-1	1.3	2.2	-3	4	1.9	+10.5	.026
10	95.2	-4	5.3	2.3	-4	5.3	2.8	-2	2.7	3.6	-5	6.7	4.6	+22.7	.057
15	142.8	-5	6.7	3.7	-5	6.7	4.2	-3.5	4.7	5.6	-7	9.3	7.2	+34	.085
20	190.4	-6	8	5	-6	8	5.5	-5	6.7	7.6	-8.5	11.3	9.2	+44.7	.112
25	238.0	-6.5	8.7	5.7	-7	9.3	6.8	-6.5	8.7	9.6	-10	13.3	11.2	+13.7x4	.137
27.5	261.8	-7	9.3	6.3	-7.5	10	7.5	-7	9.3	10.2	-11	14.7	12.6	+15.5	.155
30	285.6	-7	9.3	6.3	-8	10.7	8.2	-8	10.7	11.6	-12.5	16.7	14.6	+17	.17
32.5	309.4	-7.5	10	7	-9	12	9.5	-9	12	12.9	-13.5	18	15.9	+18.5	.185
35	333.2	-8	10.7	7.7	-9	12	9.5	-10	13.3	14.2	-14	18.7	16.6	+20	.20
37.5	357.0	-7	10.7	6.3	-10	13.3	10.8	-11	14.7	15.6	-15	20	17.9	+21.2	.212
40	380.8	-8	10.7	7.7	-10	13.3	10.8	-12	16	16.9	-16	21.3	19.2	+22.7	.227
42.5	404.6	-8	10.7	7.7	-11	14.7	12.2	-14	18.7	19.6	-18	24	21.9	+25	.25
45	428.4	-8	10.7	7.7	-12	16	13.5	-16	21.3	22.2	-20	26.7	24.6	+26.7	.267
47.5	452.2	-14	18.7	15.7	-15.5	20.7	18.2	-20	26.7	27.6	-22.5	30	27.9	+36.5	.365
50	476.0	-19	25.4	22.4	-19	25.4	22.9	-23.5	31.4	32.3	-26	34.6	32.5	-	-
0	0	-14	18.7	15.7	-12	16	13.5	-12	16	16.9	-13	17.3	15.2	(+52x4)	-
Zero Correction Factor x 10^{-3} in.		-3			-2.5			+0.9			-2.1			⇒Points averaged to determine linear curve.	
Slope Linear Curve KIPS/ 10^{-3} in.		43.1			34.3			25			20.4				

TABLE 11

U - GAGES

HYD PRESS psi x 10^2	LOAD lb. x 10^3	I GALV DIV.	I in. x 10^{-3}	I Zero corrected in x 10^{-3}	II GALV DIV.	II in. x 10^{-3}	II Zero corrected in x 10^{-3}	III GALV DIV.	III in. x 10^{-3}	III Zero corrected in x 10^{-3}	IV GALV DIV.	IV in. x 10^{-3}	IV Zero corrected in x 10^{-3}	V AV. GALV DIV.	V Axial Strain, %
5	47.6	0	0	0	+ .5	-.7	3.0	- .5	.7	2.5	-1	1.3	2	+ 8.5	.021
10	95.2	- .5	.7	.7	-1.5	2.0	5.7	-2.5	3.3	5.1	-2	2.7	3.4	+22	.055
15	142.8	-1	1.3	1.3	-3	4	7.7	-4.5	6	7.8	-3.5	4.7	5.4	+32.5	.081
20	190.4	-2	2.7	2.7	-5	6.7	10.4	-5	6.7	(8.5)	-5	6.7	7.4	+45	.112
25	238.0	-2	2.7	2.7	-6.5	8.7	12.4	-8	10.7	12.5	-6	8	8.7	+14.5x4	.145
27.5	261.8	-2	2.7	2.7	-7.5	10	13.7	-9	12	13.8	-7	9.3	10	+16	.16
30	285.6	-2	2.7	2.7	-9	12	15.7	-10	13.3	15.1	-8	10.7	11.4	+17.5	.175
32.5	309.4	-2	2.7	2.7	-10	13.3	17	-11	14.7	16.5	-9	12	12.7	+20	.20
35	333.2	-3	4	4	-11	14.7	18.4	-12.5	16.7	18.5	-10	13.3	14	+22	.22
37.5	357.0	-3	4	4	-12	16	19.7	-13.5	18	19.8	-11	14.7	15.4	+23	.23
40	380.8	-3	4	4	-13	17.3	21	-15	20	21.8	-13	17.3	18	+25	.25
42.5	404.6	-3	4	4	-15	20	23.7	-17	22.7	23.5	-14	18.7	19.4	+27	.27
45	428.4	-4	5.3	5.3	-16	21.3	25	-19	25.4	27.2	-16	21.3	22	+29.5	.295
47.5	452.2	-5	6.7	6.7	-18.5	24.7	28.4	-22	29.3	31.1	-18	24	24.7	+33	.33
50	476.0	-5	6.7	6.7	-21	28	31.7	-24	32	33.8	-20	26.7	27.4	+40x4	.40
0	0	-1	1.3	1.3	-10	13.3	17	-11	14.7	16.5	-9	12	12.7	+37x1	.092
Zero Correction Factor x 10^{-3} in.			0			+3.7			+1.8			+ .7			
Slope Linear Curve KIPS/10^{-3} in.			98			18.2			19			26.4			

] ⟹ Points averaged to determine linear curve.

( ) ⟹ Discarded points.

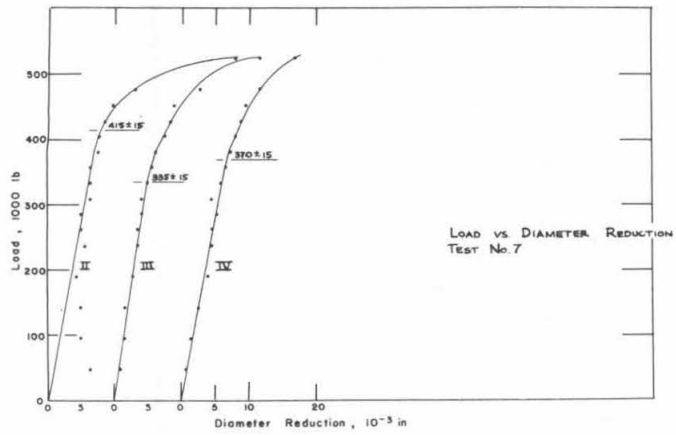

Fig. 11 Load versus diameter reduction, Test No. 7

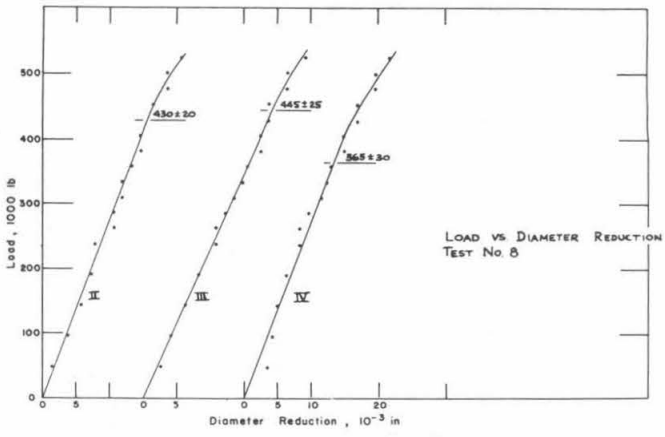

Fig. 12 Load versus diameter reduction, Test No. 8

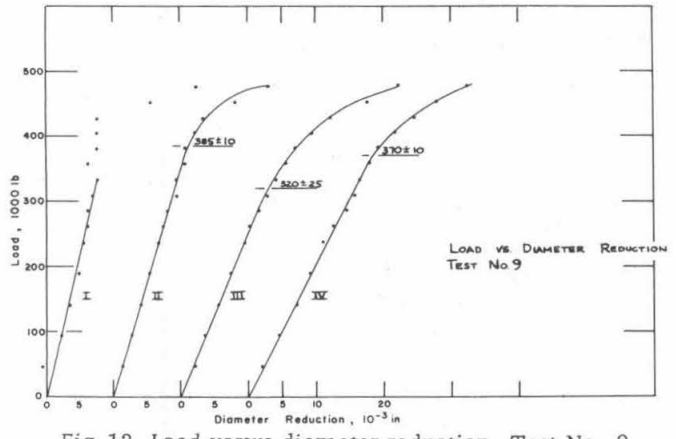

Fig. 13 Load versus diameter reduction, Test No. 9

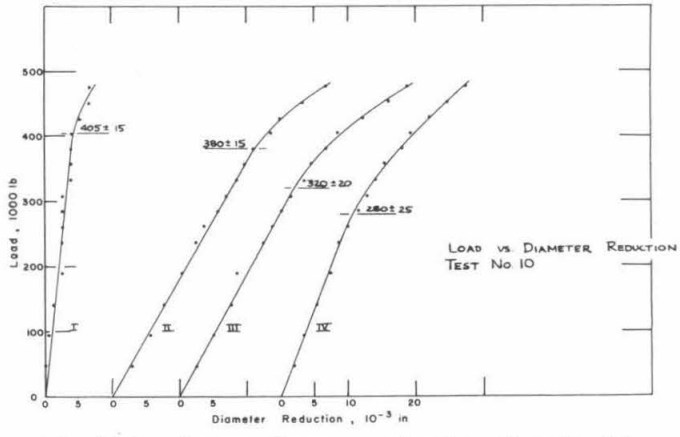

Fig. 14 Load versus diameter reduction, Test No. 10

Table 12 Summary of Test Results

Test No.	Material	Condition (Lube) (Slips)	Location of First Inelastic Deviation (inches from bottom of slips)	Load at First Inelastic Deviation x 10^3 lb.	Elastic Limit of Material psi	Load at 5×10^{-3} in. Offset; KIPS (Location)
1	4140	Best-O-Life SDL 5-1/2x5"	Up 3"	235 ± 15	--	409 Up 3"
2	4140	Best-O-Life SDL 5-1/2x5"	Up 5"	235 ± 10	--	361 Up 5"
3	Youngstown 3	Jet Lube 21 SDL 5-1/2x5"	Up 5"	300 ± 15	66,000	409 Up 5"
4	Youngstown 3	Jet Lube 21 SDL 5-1/2x5"	Up 5"	295 ± 15	66,600	413 Up 5"
5	Youngstown 4	Dry SDL 5-1/2x5"	Up 5"	345 ± 15	67,500	419 Up 5"
6	Youngstown 4	Dry SDL 5-1/2x5"	Up 5" and 10"	380 ± 20	78,000	453 468 Up 5" Up 10"
7	Youngstown 6	Dry SDXL - 5"	Up 10"	335 ± 15	70,200	470 Up 10"
8	Youngstown 6	Dry SDXL - 5"	Up 15"	365 ± 30	81,300	550 Up 15"
9	Youngstown 5	Jet Lube 21 SDXL - 5"	Up 10"	320 ± 25	70,500	414 Up 10"
10	Youngstown 5	Jet Lube 21 SDXL - 5"	Up 15"	280 ± 25	71,700	412 Up 15"

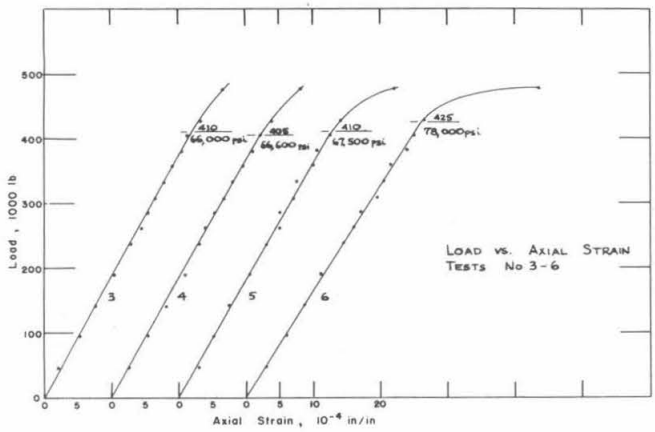

Fig. 15 Load versus axial strain, Tests 3-6

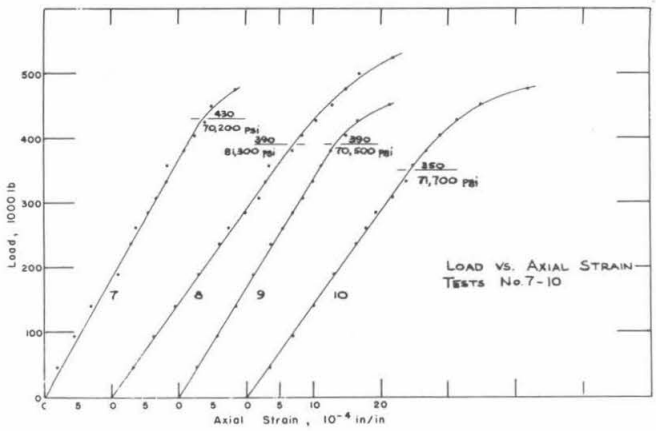

Fig. 16 Load versus axial strain, Tests 7-10

Table 13
Maximum Permanent Reduction in Diameter, 10^{-3} in.

	Test No.	Maximum Load 10^3 lb	1 Assuming unloading at slope of initial loading	2 Reading when load is removed	3 Difference in micrometer readings
SDL	3 lub.	476	11.1	--	--
	4 lub.	523.6	17.8	39.4	14.0
	5 dry	476	12.5	19.9	26.0
	6 dry	476	8.4	16.8	23.0
SDXL	7 dry	523.6	18.5	25.8	36.0
	8 dry	523.6	2.8	22.8	9.0
	9 lub.	476	13.3	16.9	19.0
	10 lub.	476	9.7	16.5	9.0

deflection reading taken when the axial pipe load was removed indicates larger values probably because some transverse load was maintained by friction between the slips and bowl. The micrometer readings are uncertain due to the relatively large variation of pipe OD. Micrometer readings taken after loading show that the reduction in pipe diameter is nonuniform around the pipe. This effect is most pronounced in the region of the gap between right and left segments of the slips. The slip markings are $1\frac{5}{8}$ in. apart in this area, and the pipe diameter across the center of the gap is 0.010 to 0.020 in. greater than the diameter measured on either side of the gap. This occurs when the pipe yields under excessive loads, and the deformation will not increase with protracted use of the pipe because the gap between segments will locate on a different area each time the slips are set. Less than 1/32 in. permanent reduction of pipe diameter occurred at the maximum load of 523,600 lb in the Youngstown pipe specimens.

The load at the elastic limit of the pipe material was higher in the second pull on each specimen. This is due to work-hardening in the pipe material, and it is modified by the reduction in area of the pipe caused by plastic deformation in the first pull. Because of work-hardening of the pipe material, smaller and smaller deformation would be produced by successive loadings to the same maximum load, if the pipe is gripped in the same region each time.

Comparison of Experimental and Calculated Values of Load and Deflection

Values of load to start yielding in 5 in. 19.5 lb/ft, grade E drill pipe were calculated and submitted to Abegg and Reinhold Company in August 1959. The calculations were based on the following assumptions:

(a) The segment of pipe in the slips is unrestrained at the top and bottom of the slips.

(b) The critical loading condition consists of the full hook load, combined with the average crushing force uniformly distributed around the circumference of the pipe.

(c) The shear distortion energy criterion for yielding is used, based on yield strength of 75,000 psi.

(d) API taper on slips and bowls.

The experimental values of load to start yielding in the slip area provide a check on the calculations and therefore a check on the validity of the assumption used.

A plot of yield load versus transverse load factor is presented in Fig.17 on which the experimental points and the calculated curve appear. The experimental points are plotted assuming a coefficient of friction of 0.5 for a dry bowl, and a coefficient of 0.06 for a lubricated bowl. Values of load at the offset deflection of 0.005 in. are also plotted in Fig.17. The calculated curve falls within the spread of the experimental points.

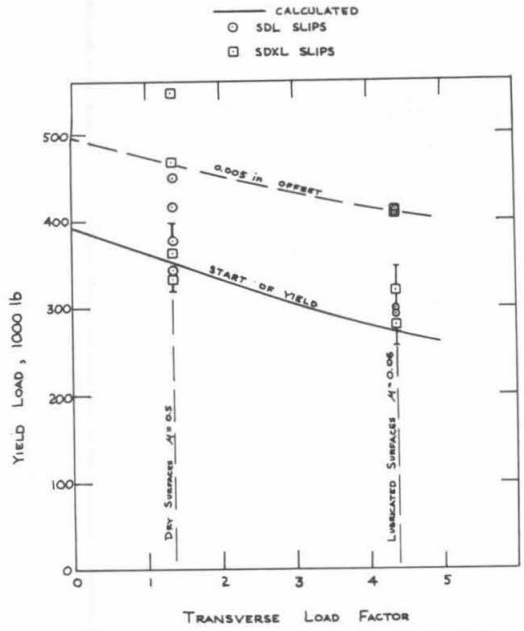

Fig. 17 Yield load versus transverse load factor

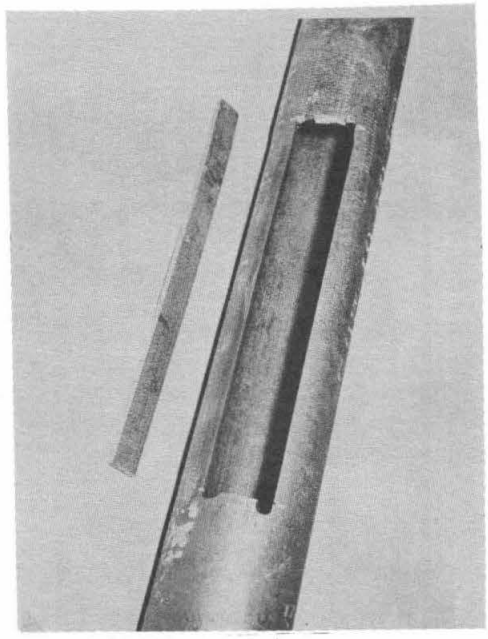

Fig. 18 Pipe specimen No. 3

A more valid comparison between calculated and experimental values may be made when the experimental values are adjusted to an elastic limit (start of inelastic deformation) value of 75,000 psi. Such an adjustment moves the experimental points in Fig.17 upward. The actual load to start yielding in the pipe is an unknown amount less than the load which produces a measurable amount of inelastic deformation. An adjustment for this effect moves the experimental points in Fig.17 downward. These two adjustments tend to compensate each other, and no correction is made in Fig. 17. The agreement between calculated and experimental values of yield load is very good.

The change in inside diameter of the pipe may be calculated and compared to the measurements. It is assumed that the pipe behaves elastically. The circumferential strain in the pipe is given by

$$\epsilon_\theta = \frac{\sigma_\theta}{E} - \mu\frac{\sigma_a}{E}$$

where

σ_θ = circumferential stress
σ_a = axial stress
E = Young's modulus
μ = Poisson's ratio

The stresses at the pipe ID are given by

$$\sigma_\theta = -\frac{2b^2p}{b^2-a^2}$$

and

$$\sigma_a = P/A$$

where

b = outside radius of pipe
a = inside radius of pipe
p = external pressure on pipe (varies through slip area)
P = axial load (varies through slip area)
A = cross-sectional area

The deflection at the pipe ID is then

$$\delta = 2a\ \epsilon_\theta = -\frac{2a}{E}\left(\frac{2b^2p}{b^2-a^2} + \frac{P}{A}\right)$$

If we let $p = KP/A_L$ where K is the transverse load factor, and A_L is the slip area

$$\delta = -\frac{2a}{E}\ \frac{P}{A}\left(\frac{2b^2}{b^2-a^2}\ \frac{KA}{A_L} + \mu\right)$$

The negative sign, indicating a reduction in pipe diameter, will be dropped in the following discussion.

Below the slips where p = K = 0, and P is the total applied force,

$$\delta = \frac{2\mu aP}{EA}$$

and the slope of the elastic portion of the load versus deflection relation is $EA/2\mu a = 1.23 \times 10^8$ lb/in. for 5 in., 19.5 lb/ft steel drill pipe.

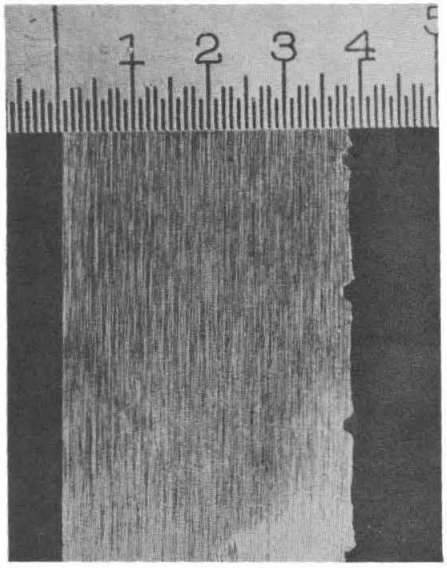

Fig. 19 Profile of slip markings from upper section of gripped area, specification No. 3

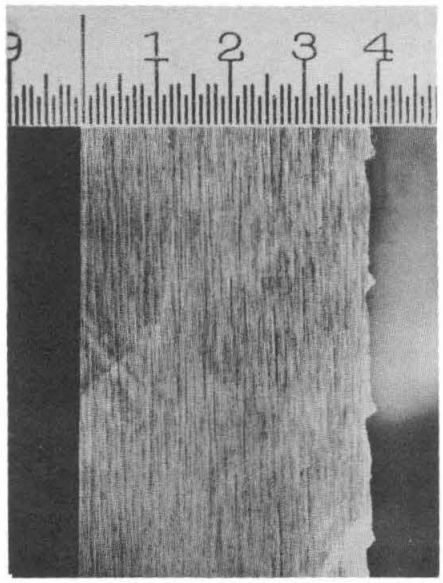

Fig. 20 Profile of slip markings from lower section of gripped area, specification No. 3

The measured slope averaged over all tests was approximately 0.65×10^8 lb/in. at the bottom of the slips, indicating that some external pressure is applied at that point. (This is also indicated by slip markings.)

The tests with the SDL slips show that the P versus δ curve with the least slope is either 5 or 10 in. above the bottom of the slips, while with the SDXL slips the slope 10 or 15 in. above the bottom of the slips is smaller. This indicates that the peak lateral pressure in the SDXL slip occurs in a higher region than in the SDL slips, and agrees with the observations of slip markings (discussed below) and the location of the first inelastic deformation.

A more detailed analysis of the slopes of the experimental P versus δ curves could be made. It is believed that such an analysis will not give significant information because:

(a) Some of the slopes are inaccurate due to malfunction of the displacement gages in several tests.

(b) Some of the displacement gages were inoperative, particularly those located in the lower slip area.

(c) High spots in the pipe, and out-of-round pipe sections tend to confuse the data, since the displacement gages measure only across one diameter.

(d) Reduction in pipe diameter is non-uniform around the pipe circumference and it is not known how the displacement gages were located with respect to the gaps between slip segments.

SLIP MARKINGS

The slip markings on the pipe are nonuniform in some areas, probably indicating initially out-of-round sections, which are forced into a round shape by the slips. This produces nonuniform lateral pressures and bending in the wall of the pipe, but should have only a slight influence on the yield load determined by measurements of the pipe ID. Nonuniform markings would also be produced if the gripping surfaces are not accurately disposed on a cylindrical surface.

A segment of slip marked pipe was cut from specimen No.3, and ground to show the profile of the slip markings. Fig.18 shows the pipe specimen, and Figs.19 and 20 show the profile of the slip markings at a magnification of approximately 8 x. The slip markings in the upper section of the gripped area are symmetrical as shown in Fig. 19. The slip markings in the lower sections of the gripped area, Fig.20, show a pile-up of metal which occurred when the pipe elongated. The maximum depth of the slip markings was measured to be 0.013 in. or 3.35 per cent of the wall thickness.

CONCLUSIONS

The following conclusions are drawn from the test results:

1 Under similar conditions pipe held in SDL and SDXL slips exhibits inelastic deformation at essentially the same load.

2 Higher loads are required to produce in-

elastic deformation with SDL and SDXL slips when the bowls are dry rather than lubricated.

3 An increase in load of 100,000 lb over the yield load produces less than 0.005 in. permanent deformation with SDL and SDXL slips in lubricated bowls.

4 Loads of 523,600 lb produce less than 1/32 in. permanent reduction in diameter with SDL and SDXL slips.

5 SDXL slips produce relatively high transverse loading in the upper slip area.

6 The yield load is satisfactorily predicted by an approximate stress analysis.

The test results show that 5-in, 19.5-lb/in. grade E drill pipe may be gripped in VARCO SDL and SDXL slips without producing excessive deformation at loads up to 500,000 lb. If slips or bushings are worn, a concentration of transverse loading can occur to increase deformation markedly. The greater back-up area of SDXL slips will maintain a more accurate taper under protracted use at high loads.

ACKNOWLEDGMENTS

We are very appreciative of the assistance rendered by Jack Reed of the Humble Oil and Refining Company; Marvin T. Parker of Great Western Drilling Company; and Charles E. Downey, Field Engineer, Youngstown Sheet and Tube Company. All drill-pipe specimens used in this work were donated by Youngstown Sheet and Tube Company.